Journal of Controlled Release 363 (2023) 101–113

Contents lists available at ScienceDirect

Journal of Controlled Release

journal homepage: www.elsevier.com/locate/jconrel

Control of cell penetration enhancer shielding and endosomal escape-kinetics crucial for efficient and biocompatible siRNA delivery

Alessio Malfanti [a,1], Haider Sami [b,1], Anna Balasso [a], Giulia Marostica [b], Busra Arpac [a], Francesca Mastrotto [a], Giuseppe Mantovani [c], Elisa Cola [b], Martina Anton [d], Paolo Caliceti [a], Manfred Ogris [b,*], Stefano Salmaso [a,*]

[a] Department of Pharmaceutical and Pharmacological Sciences, University of Padova, Via F. Marzolo 5, Padova 35131, Italy
[b] University of Vienna, Faculty of Life Sciences, Department of Pharmaceutical Sciences, Laboratory of Macromolecular Cancer Therapeutics (MMCT), Josef-Holaubek-Platz 2, Vienna 1090, Austria
[c] School of Pharmacy, University of Nottingham, Nottingham NG7 2RD, UK
[d] Institute of Molecular Immunology, School of Medicine, Technical University of Munich, Munich, Germany

ARTICLE INFO

Keywords:
Lipoplex engineering
Oligo-cationic condensing lipids
Cell penetration enhancers
Endosomal escape

ABSTRACT

Although cationic liposomes are efficient carriers for nucleic acid delivery, their toxicity often hampers the clinical translation. Polyethylene glycol (PEG) coating has been largely used to improve their stability and reduce toxicity. Nevertheless, it has been found to decrease the transfection process. In order to exploit the advantages of cationic liposomes and PEG decoration for nucleic acid delivery, liposomes decorated with tetraArg-[G-1]-distearoyl glycerol (Arg_4-DAG) dendronic oligo-cationic lipid enhancer (OCE) and PEG-lipid have been investigated. Non decorated or OCE-decorated lipoplexes (OCE_{free}-LPX and OCE-LPX, respectively) were obtained by lipid film hydration using oligonucleotide (ON) solutions. PEG and OCE/PEG decorated lipoplexes (PEG-OCE_{free}-LPX and PEG-OCE-LPX, respectively) were obtained by post-insertion of 2 or 5 kDa PEG-DSPE on preformed lipoplexes. The OCE decoration yielded lipoplexes with size of about 240 nm, 84% loading efficiency at 10 N/P ratio, ten times higher than OCE_{free}-LPX, and prevented the ON release when incubated with physiological heparin concentration or with plasma. The PEG decoration reduced the zeta potential, enhanced the lipoplex stability in serum and decreased both hemolysis and cytotoxicity, while it did not affect the lipoplex size and ON loading. With respect to OCE_{free}-LPX, the OCE-LPX remarkably associated with cells and were taken up by different cancer cell lines (HeLa and MDA-MB-231). Interestingly, 2 or 5 kDa PEG decoration did not reduce either the cell interaction or the cell up-take of the cationic lipoplexes. With siRNA as a payload, OCE enabled efficient internalization, but endosomal release was hampered. Post-transfection treatment with the lysosomotropic drug chloroquine allowed to identify the optimal time point for endosomal escape. Chloroquine treatment after 12 to 20 h of LPX pre-incubation enabled siRNA mediated target knockdown indicating that this is the time window of *endo*-lysosomal processing. This indicates that OCE can protect siRNA from lysosomal degradation for up to 20 h, as shown by these rescue experiments.

1. Introduction

Over the last decades, oligonucleotides (ONs) have been emerging as powerful therapeutic tools to selectively target a variety of genetic disorders including cystic fibrosis, muscular dystrophy, cardiovascular disorders, infectious diseases and cancer [1]. In 2013, the approval of the first ON for treatment of hypercholesterolemia, Kynamro® raised great enthusiasm for this class of therapeutics. Currently, 15 oligonucleotides have been granted new drug approval (NDA) by U.S. Food and Drug Administration (FDA) and one by EMA [2,3]. However, while "gapmers technology" used to develop Kynamro® provides stable ASOs, efficient delivery of nucleic acid drugs to specific targets and the minimization of side effects, including immune system activation, are still open challenges.

* Corresponding authors.
E-mail addresses: m.ogris@univie.ac.at (M. Ogris), stefano.salmaso@unipd.it (S. Salmaso).
[1] Alessio Malfanti, Haider Sam: provided equal contribution

https://doi.org/10.1016/j.jconrel.2023.09.022
Received 16 March 2023; Received in revised form 21 July 2023; Accepted 14 September 2023
Available online 26 September 2023

In this realm, anticancer ONs have been largely investigated [4] and, although none has been approved yet, 88 candidates are currently in clinical phase 1, 2 or 3 (ClinicalTrials.gov). However, ON delivery represents the major hurdle limiting their clinical translation [5]. Therefore, there is an unmet need of innovative, and safe delivery strategies that allow for cancer cell targeting and efficient transfection.

Although viral vectors are efficient nucleic acid delivery systems, their clinical exploitation suffers from their immunogenicity and activation of inflammation reactions. Instead, non-viral vectors are poorly immunogenic carriers with high loading capacity and scalability of production [6]. Among non-viral vectors, cationic nanoparticles, including lipoplex forming liposomes, have been the most used carriers for ON delivery [7,8]. Oligocationic excipients may have a crucial role in the delivery of nucleic acids, because they combine the nucleic acid condensing ability (loading and stabilization) with the biobarrier penetration (typically, intracellular delivery), which is one of the requisites for delivery to the molecular targets of this class of therapeutic molecules. These effects are expected to depend on their chemical composition and architecture [9–12]. However, the structure of the components of the delivery systems may also affect the nucleic acid endosomal escape, which is a requisite for transfection activity [13,14,53]. Therefore, the therapeutic performance of these formulations may be correlated to the chemical composition and structure, i.e. linear or dendronic, of these components. On the other side, cationic nanosystems display dose-dependent toxicity by inducing cell lysis, necrosis, immune system activation and systemic release of pro-inflammatory factors, which can also depend on the chemical composition and structure of these materials [15]. The combination of oligocationic components with excipients that counterbalance the side effects stemming from the positive charge of the resulting particles is required. PEG coating has been found to ameliorate the cytotoxic and stability profile of cationic liposomes and nanoparticles, reduce their opsonization and enhance the in vivo behavior. However, the beneficial effect in reducing the cell toxicity may contrast with the nucleic acid condensation and cell penetration of the system [16]. Therefore, it is important to get information about the nanoparticle composition to establish the optimal combination of excipients to orchestrate efficient nucleic acid delivery.

In order to optimize the delivery of ON, cationic carriers must be designed by fine tuning the surface properties that minimize opsonization and cytotoxicity while allowing for cell interaction and uptake balancing. Accordingly, PEG with selected physicochemical properties and cationic moieties with double function as ON condensing agents and cell up-take promoters can be properly combined to yield efficient ON delivery systems [17].

After cell entry, the endosomal escape represents the last biobarrier for nanocarriers reaching the cytoplasm. In this regard, small molecules timely triggering the endosomal escape can be exploited to facilitate the nanocarrier trafficking towards cytosolic targets [18].

Aimed at investigating the effect of non-linear and non-peptidic oligocationic materials on ON delivery and transfection, we generated lipoplexes decorated with a synthetic arginine-rich lipid terminated oligo-cationic dendronic enhancer (OCE) as ON condensing agent and cell penetration promoter. The oligo-cationic OCE used in this work was previously found to enhance intracellular delivery of colloidal carriers and macromolecules [19,20]. With respect to linear Arg rich peptides, synthetic cell penetration enhancers have higher stability to proteases and do not elicit biological effects. A small library of lipoplexes decorated with the OCE and PEG at different molar ratio was produced to investigate the correlation of the surface composition with the biopharmaceutical performance of the formulations. Furthermore, a fine tuning of the cell treatment modalities with endosomal escape inducing agents was conducted to investigate the timeline of intracellular processing of the delivered ONs.

2. Materials

Hydrogenated soy phosphatidylcholine (HSPC) was purchased from Lipoid GmbH (Ludwigshafen, Germany). 1,2-distearoyl-sn-glycero-3-phosphoethanolamine-N-[methoxy(polyethylene glycol)-2000] [mPEG $_{2kDa}$-DSPE] was obtained from Laysan Bio (Arab, AL, USA) and 1,2-distearoyl-sn-glycero-3-phosphoethanolamine-N-[methoxy(polyethylene glycol)-5000] [mPEG$_{5kDa}$-DSPE] was purchased from JenKem Technology (Plano, TX, USA). All buffer salts, solvents and reagents were purchased from VWR International PBI (Radnor, PA, USA) and Sigma-Aldrich (St. Louis, MO, USA).

Cy3-dsDNA and dsDNA (19 bp) were obtained from Biomers GmbH (Ulm, Germany). All siRNAs used in this work were kindly supplied by GlaxoSmithKline (GSK, UK): 1) siRNA for gene knockdown of firefly luciferase (anti-luc siRNA; sense strand sequence 5′-CUUACGCUGAGUACUUCGAdTdT-3′; two phosphorothioate bonds on the 3′ terminus of sense strand and one on 3′ terminus of antisense strand), 2) siRNA employed as negative or scrambled control (control siRNA; sense strand sequence 5′-AUCGUACGUACCGUCGUAUdTdT-3′; two phosphorothioate bonds on the 3′ terminus of both sense and antisense strands), and 3) fluorescently labelled siRNA (AF647-siRNA; AF647 coupled to 3′ terminus of the sense strand of negative control siRNA).

Foetal bovine serum (FBS), penicillin (10,000 IU/mL), streptomycin (10 mg/mL), L-glutamine (200 mM), sterile Dulbecco's phosphate buffered saline (PBS), Dulbecco's Modified Eagle's Medium-high glucose, MTT assay, and all other reagents for cell-culture studies were purchased from Sigma-Aldrich (St. Louis, MO, USA). Wheat Germ Agglutinin-Alexa Fluor 488 conjugates (WGA-Alexa Fluor 488) TrypLE Express, Versene, SYBR Safe DNA gel stain and Quant-iT PicoGreen dsDNA Assay Kit were purchased from Thermo Fisher Scientific (Madison, WI, USA). Water was purified with a Sartorius AriumPro system (Germany) for preparing nucleic acid solutions. Passive lysis buffer was purchased from Promega (Germany).

3. Methods

3.1. Lipoplexes preparation

3-(4-(12,17-diamino-4-(((3-(2-amino-5-guanidinopentanamido)-2-((2-amino-5-guanidinopentanamido) methyl)-2-methylpropanoyl)oxy) methyl)-8-((2-amino-5-guanidinopentanamido)methyl)-17-imino-4,8-dimethyl-3,7,11-trioxo-2,6-dioxa-10,16-diazaheptadecyl)-1H-1,2,3-triazol-1-yl)propane-1,2-diyl distearate (Arg_4-DAG) was synthesized using a procedure reported in literature with modifications [20] (Supporting Information: Scheme S1–3, Fig. S1–6). Lipoplexes were prepared by thin layer hydration technique using a 2:1 hydrogenated soy phosphatidylcholine (HSPC)/cholesterol molar ratio and 4 mol% of Arg_4-DAG (OCE) with respect to lipids [21]. Briefly, 5 mg of lipids containing 4 mol% of OCE were dissolved in 1.5 mL chloroform and the organic solvent was then removed under reduced pressure by rotavapor to generate a lipid film that was then hydrated with 400 μL of 10 mM HEPES, 0.15 M NaCl at pH 7.4 or 400 μL of dsDNA or siRNA solutions in the same buffer. The concentration range of dsDNA or siRNA solutions used for hydration was 16.7–167 μM in order to yield decreasing nitrogen to phosphate (N/P) ratio from 10 to 1. The lipoplexes underwent 60 s of sonication with an Ultrasonic Homogenizer (Omi International, Kennesaw, GA, USA) set at 20% power and extruded 11 times through a 200 nm cut-off polycarbonate membrane. Lipoplexes were then diluted to the final concentration of 5 mg/mL using the same buffer. The lipoplex formulations containing the OCE (*OCE-LPX*) were incubated at 37 °C for 1 h and dialyzed for 24 h against 2 L of 10 mM HEPES, 0.15 M NaCl at pH 7.4 by using a Float-A-Lyzer® G2 with 300 kDa MWCO to remove unloaded dsDNA.

OCE-free lipoplexes were also prepared as control formulations using the same procedure (*OCE_{free}-LPX*). OCE-containing and OCE-free lipoplexes loaded with dsDNA or siRNA at 10 N/P ratio were then

decorated with increasing ratio of PEG_{2kDa}-DSPE (PEG_{2kDa}) or PEG_{5kDa}-DSPE (PEG_{5kDa}) in the 0–5 mol% range with respect to lipids by 10 min incubation at 37 °C.

Lipoplexes were also generated by functionalization of liposomes with OCE using a post-insertion technique to investigate the effect of complexation with dsDNA on preformed cationic liposomes and the OCE/dsDNA interaction profile by microcalorimetric analysis. To this aim, plain liposomes obtained by lipid film hydration of a 2:1 mol/mol HSPC/Cholesterol mixture were used to prepare formulations in which 4 mol% of OCE with respect to the lipids was post-inserted in the lipid bilayer by 1 h incubation at 37 °C with liposomes (*OCE_{post}-LIP*). To study the effect of complexation with dsDNA on preformed cationic liposomes, dsDNA was added in different amounts to the OCE_{post} -LIP suspensions to yield 1–10 N/P ratios and formulations were incubated at 37 °C for additional 30 min before the dialysis step that was performed to remove the unbound dsDNA using Float-A-Lyzer® G2 with 300 kDa MWCO resulting in lipoplexes (*OCE_{post}-LPX*).

Lipoplexes for cell uptake studies were also prepared using a fluorescently labelled Cy3-dsDNA (Biomers, Ulm, Germany) or AF647-siRNA.

Preliminary studies with ON free liposomes obtained with both procedures (hydration of lipid mixture containing the OCE and post-insertion of OCE on plain liposomes) at increasing OCE/lipid ratio in the 1–10 mol% range generating OCE-LIP and OCE_{post}-LIP, respectively, were performed.

The quantification of OCE associated to the liposome formulations after dialysis was performed by Sakaguchi assay [22] upon liposome disaggregation with a 1% *v*/v Triton X-100 aqueous solution on the basis of a calibration line obtained with Arg_4-DAG in 1% v/v Triton X-100 aqueous solution ($y = 12.4819\times + 0.0163$, $R^2 = 0.9971$). Validation of the dialysis process of Arg_4-DAG was performed using a solution of 0.64 mg/mL Arg_4-DAG in 10 mM HEPES, 0.15 M NaCl at pH 7.4.

The quantification of PEG associated to liposomes was performed after isolation of liposomes (1 mL aliquots) by centrifugation for 30 min at 14,000 rpm (Sigma 1–14 Microfuge, Newtown, UK). Then, the supernatants were recovered and the PEG concentration was assessed by iodine assay [23]. The supernatants were also analysed for lipid concentration by Stewart assay to evaluate the efficiency of liposome isolation by centrifugation [24].

3.2. Dynamic light scattering and nanoparticle tracking analysis

Size, polydispersity and zeta potential of liposomes and lipoplexes was assessed by Dynamic Light Scattering (DLS) using a Malvern NanoZS Zetasizer (Malvern Panalytical Ltd., Malvern, UK). Liposomes and lipoplexes were diluted to the concentration of 0.2 mg/mL in 10 mM HEPES, 0.15 M NaCl, pH 7.4 before the size analysis and in 5 mM HEPES pH 7.4 for the zeta potential analysis. For nanoparticle tracking analysis (NTA) measurements, samples were diluted in in 10 mM HEPES, 0.15 M NaCl, pH 7.4 at a 10^8–10^9 particles/mL concentration range, as reported elsewhere [25] and measured with Nanosight NS500 (Malvern Panalytical, Malvern, UK) equipped with 488 nm laser. The size was expressed as z-average for DLS measurements and as mean values for NTA.

3.3. Lipoplexes loading capacity and efficiency

The ON loading in the lipoplexes was quantified by spectrofluorimetric analysis upon disaggregation of Cy3-dsDNA-loaded lipoplexes with 1% *v*/v Triton X-100 aqueous solution and dilution with 10 mM HEPES, 0.15 M NaCl at pH 7.4 using a LS 50 B Perkin-Elmer fluorimeter (Waltham, MA, USA) with an excitation wavelength of 554 nm and emission of 568 nm. The concentration of Cy3-dsDNA in the samples was derived from a calibration curve obtained by serial dilutions of a 100 μM Cy3-dsDNA solution in 10 mM HEPES, 0.15 M NaCl at pH 7.4 ($y = 64.017\times + 1.8557$. $R^2 = 0{,}9993$). The Cy3-dsDNA encapsulation efficiency in liposomes was reported as the percentage of loaded Cy3-dsDNA after liposome dialysis with respect to the Cy3-dsDNA used for lipid film hydration. The liposome loading capacity was reported as the amount of encapsulated Cy3-dsDNA assessed after dialysis with respect to lipids (μg Cy3-dsDNA /mg lipids).

For siRNA quantification, picogreen based assay was used as both luciferase siRNA (luc siRNA; for knockdown of luciferase gene) and scrambled negative control siRNA (NC siRNA; with scrambled non-coding sequence) were not fluorescently labelled. Luc and NC siRNA were diluted in TE buffer (10 mM Tris HCl and 0.1 mM EDTA, pH 7.4) to generate concentrations in the 0.001–1 μg/mL range to create calibration curves via picogreen assay, which were then employed to estimate the siRNA loading in tested lipoplex formulations. To investigate the interference from Triton X-100, calibration curves were prepared with and without Triton X-100. The readout was done in a black F-bottom 96-well plate by employing Infinite 200 pro Tecan plate reader with excitation wavelength of 480 nm and emission wavelength of 532 nm. The siRNA encapsulation efficiency in liposomes was reported as the percentage of loaded siRNA after liposome dialysis with respect to the siRNA used for lipid film hydration. The liposome loading capacity was reported as the amount of encapsulated siRNA assessed after dialysis with respect to lipids (μg siRNA/mg lipids).

3.4. Isothermal titration calorimetry

The thermodynamics of the interaction between dsDNA and OCE coated liposomes, prepared by post-insertion procedure, was investigated by isothermal titration calorimetry (ITC) using a Malvern MicroCal, LLC VP-ITC microcalorimeter system (Malvern - UK). For each set of measurements, a 20 μM dsDNA solution in Milli-Q water was placed in the syringe and used to titrate 1.5 mL of an aqueous suspension of 2.7 mg/mL OCE_{post}-LIP (corresponding to 172.7 μM of OCE) or OCE_{free}-LIP. The titration was performed in order to span a 227–8 N/P ratio range. The reference cell was filled with 1.5 mL of Milli-Q water. The analysis was performed at 25 °C, with an agitation speed of 351 rpm, by 28 repetitive dsDNA injections of 10 s at intervals of 200 s. The analysis was also performed in 10 mM HEPES pH 7.4, in 10 mM HEPES pH 7.4 with 0.15 M NaCl and in 10 mM HEPES pH 7.4 with 0.3 M NaCl in order to elucidate the dsDNA/OCE electrostatic interaction in the presence of salts. All measurements were replicated three times and data processing was performed with the Microcal Origin 3.5 software.

3.5. Heparin displacement assay

The displacement of dsDNA from lipoplexes by heparin was investigated by polyacrylamide gel electrophoresis. Ten μL of OCE-LPX and OCE_{free}-LPX formulations loaded with dsDNA at 10 N/P ratio containing 30 pmol of dsDNA were mixed with 2 μL of aqueous heparin solutions at increasing concentrations (0.15–10 UI/mL). The samples were incubated for 15 min and then added of 3 μL of loading buffer containing 0.25% xylene cyanol in a 50% *v*/v glycerol/water mixture. The equivalent of 30 pmol free dsDNA and lipoplexes without heparin (0 UI/mL) were used as controls. The samples were loaded in 12% polyacrylamide gel and run for 1 h at 100 V with 100 mM Tris, 100 mM boric acid, 2 mM EDTA (TBE) buffer, pH 7.8. Afterwards, the gel was gently shaken for 30 min in a staining medium containing GelRed® Nucleic acid Gel Stain 10,000 X (Biotium, Fremont, CA). Finally, the gel was imaged by using a Perkin Elmer UV-Transilluminator Geliance 600 Imaging System (Perkin Elmer, Shelton, CT, USA).

3.6. Lipoplexes stability study

The colloidal stability of dsDNA loaded OCE-free lipoplexes (*OCE_{free}-LPX*) prepared at 10 N/P ratio, OCE-LPX at 5 and 10 N/P ratio, and OCE-LPX at 10 N/P ratio decorated with 2.5 or 5 mol% of $mPEG_{2kDa}$-DSPE or $mPEG_{5kDa}$-DSPE (*OCE-LPX/2.5PEG_{2kDa}*, *OCE-LPX/5PEG_{2kDa}*, *OCE-LPX/*

2.5PEG$_{5kDa}$, OCE-LPX/5PEG$_{5kDa}$) was tested by incubation in buffer (10 mM HEPES, 0.15 M NaCl, pH 7.4) at 37 °C and in cell culture media supplemented with 10% foetal bovine serum (DMEM+10%FBS) at 37 °C by measuring the size with DLS analysis at scheduled time points.

3.7. Stability in rat plasma

The stability of the OCE-LPX/5PEG$_{5kDa}$ formulation loaded with dsDNA at 10 N/P ratio was tested in rat plasma by gel electrophoresis. Ten μL of lipoplexes at 5 mg/mL concentration in 10 mM HEPES, 0.15 M NaCl pH 7.4 were incubated at 37 °C with 10 μL of whole rat plasma for 24 h. At scheduled timepoints, 10 μL of these mixtures was added of 3 μL of water. After 15 min of incubation at 37 °C the samples were added of 3 μL of a 0.25% xylene cyanol solution in a 50% *v*/v glycerol/water mixture and loaded on 12% acrylamide gel. The gel was run for 1 h at 100 V in TBE buffer, pH 7.8 and stained by 30 min gentle shaking in Milli-Q water with GelRed® Nucleic acid Gel Stain 10,000 X (Biotium, Fremont, CA). The images were recorded using a Perkin Elmer UV-Transilluminator Geliance 600 Imaging System (Perkin Elmer, Shelton, CT, USA). A control sample was generated by adding 10 μL of the OCE-LPX/5PEG$_{5\ kDa}$ formulation of 3 μL of a 500 IU/mL heparin aqueous solution and tested as reported above to confirm the dsDNA displacement.

3.8. Cell culture and transduction

MDA-MB-231 (ATCC, VA, USA), MCF7 and HeLa (ECACC, UK) cells were grown at 37 °C in DMEM medium supplemented with 10% of heat-inactivated fetal bovine serum (FBS), 2 mM L-glutamine, 100 IU/mL penicillin and 100 μg/mL streptomycin, under 5% CO_2 atmosphere. The cells were sub-cultured at about 70–80% confluency by 5 min treatment with a 0.05% (*w/v*) trypsin, 0.02% (w/v) EDTA solution (Sigma Aldrich, St. Louis, MO, USA) in PBS or TrypLE™ express at 37 °C and seeded at the appropriate cell concentration. To obtain tumor model cell lines for siRNA knockdown studies, cells expressing EGFP-Luciferase fusion protein under a constitutively active phosphoglycerol promoter PGK from three different cell types were lentivirally transduced with PGK-EGFP-Luc, as reported previously [26], and were designated as MDA-MB-231-PGK-EGFP-Luc, MCF7-PGK-EGFP-Luc and HeLa-PGK-EGFP-Luc respectively.

3.9. Cytotoxicity MTT assay

MDA-MB-231 cells were seeded on a 96-well plate at a density of 1×10^4 cells per well. After 24 h, the cell culture medium was discarded, the cells washed twice with PBS and then incubated with 200 μL of lipoplex suspensions in complete medium. Three dsDNA concentrations (50, 125 and 250 nM) were tested for each liposomal formulation. After 24 h of incubation, the medium was removed, the cells washed three times with PBS and then 200 μL of complete medium containing 20 μL of a 5 mg/mL MTT solution in PBS was added per well. After 3 h of incubation at 37 °C, the medium was discarded and 200 μL of DMSO was added to each well. The plate was maintained under gentle stirring for 30 min before spectrophotometric absorbance was measured at 570 nm using a microplate reader (Bio-Teck Instrument, Winooski, VT, USA). The results were reported as percentage of cell viability with respect to untreated cells.

3.10. Hemolysis assay

Ten mL of rat blood were centrifuged in a BD Vacutainer tube with sodium citrate (BD, Franklin Lakes, NJ, USA) at 2,250 rpm for 5 min. The plasma was discharged and replaced with 0.9% NaCl solution. Then, after three washing-centrifugation cycles of the red blood cells (RBCs), the supernatant was replaced with PBS, pH 7.4. *OCE-LPX, OCE-LPX/2.5PEG$_{2kDa}$, OCE-LPX/5PEG$_{2kDa}$, OCE-LPX/2.5PEG$_{5kDa}$, OCE-LPX/5PEG$_{5kDa}$* loaded with dsDNA at 10 N/P ratio and the control OCE-free formulations (OCE$_{free}$-LPX/2.5PEG$_{2kDa}$, OCE$_{free}$-LPX/5PEG$_{2kDa}$, OCE$_{free}$-LPX/2.5PEG$_{5kDa}$, OCE$_{free}$LPX/5PEG$_{5kDa}$) were incubated with RCBs at liposome concentrations in the 0.05–0.3 mg/mL range. The test was also performed by using 1% *v*/v Triton X-100) as positive control (100% hemolysis) and PBS as negative control. All the samples were incubated for 1 h at 37 °C and then centrifuged for 5 min at 2,250 rpm. One hundred μL of supernatant was transferred on a 96-wells plate and the absorbance of released hemoglobin was spectrophotometrically measured by a microplate reader at 570 nm (Bio-Teck Instrument, Winooski, VT, USA).

3.11. Flow cytometric analyses

Cell association of lipoplexes was investigated in MDA-MB231 and HeLa cells by flow cytometry. Cells were seeded into a transparent 24-well plate at a density of 100,000 cells/well for HeLa and 50,000 cells/well for MDA-MB231 and incubated for 24 h before lipoplex treatment at 37 °C, 5% CO_2. Lipoplexes loaded at 10 N/P ratio were prepared as previously described, but encapsulating AF647-labelled siRNA for tracking via flow cytometry. Cells were treated with different lipoplex formulations at siRNA concentration of 50 nM (corresponding to 10 pmol siRNA per well) either for 1 h or 24 h and then the treatment medium was removed, and the cells were washed three times with warm PBS. Cells were then detached with 60 μL of TryPLE and harvested in two steps for high cell recovery. In the first step, the resulting cell suspension was transferred into a 96-well plate. Afterwards, in the second harvesting step, the wells were washed with 100 μL of PBS (containing Versene solution) to recover all the remaining cells, and the suspension was transferred in the corresponding well of the plate. The cell suspension was then carefully suspended and analysed through flow cytometry by MACSQuant Analyzer 10 (Miltenyi Biotech, Germany). Cells were stained with DAPI for live-dead analysis (V1-A channel, exc.λ 405 nm, em. λ 450/50 nm band pass filter). AF647-siRNA fluorescence was measured in the R1 channel (exc. λ 635 nm, em. λ 693/38 nm band pass filter). During the whole measurement, cells were maintained at 4 °C. Post-acquisition, data analysis was performed with FlowJo software v. 10.8.1.

3.12. Confocal microscopy

Twelve mm diameter confocal microscopy round coverslips (Thermo Fisher Scientific, Madison, WI, USA) placed on a 24-well plate were treated for 1 h with 300 μL each of a 0.2 mg/mL sterile solution of poly-D-lysine in Milli-Q water at room temperature. Wells were rinsed three times with PBS and then MDA-MB-231 cells were seeded at a density of 1.5×10^5 cells/well in complete medium. The cells were grown for 24 h and then the medium was discarded and replaced with 200 μL of lipoplexes in complete medium at the concentration of 125 nM of Cy3-dsDNA or AF647-siRNA. After 1 h incubation, cells were gently washed twice with 200 μL of PBS added of 10% FBS and then twice with 200 μL of PBS and fixed by 20-min treatment with 200 μL/well of 4 *w/v* % paraformaldehyde in PBS. The staining of the cell nucleus was performed by a 10 min incubation with a 200 μL/well of DAPI solution in PBS (5 μg/mL), whereas cell membranes were fluorescently labelled by a 10 min incubation with 200 μL of a 5 μg/mL Wheat Germ Agglutinin-AlexaFluor 488 conjugate solution in PBS. The coverslips were mounted on glass slides using Mowiol® (Sigma Aldrich, St. Louis, MO, USA) as mounting medium. Cell samples were imaged with a Zeiss LSM 800 confocal microscope (Jena, Germany) using an immersion lens with a magnification of 63×. Lasers with excitation wavelengths at 405, 488, and 561 or 640 nm were used to detect DAPI, WGA-AlexaFluor 488, and Cy3-dsDNA or AF647-siRNA, respectively.

3.13. Release studies

A 1.5 mL volume of lipoplexes loaded with Cy3-dsDNA at 10 N/P

ratio (1 μM Cy3-dsDNA) was transferred in a Float-A-Lyzer with a cut-off of 300 kDa and dialyzed against 2 L of 10 mM HEPES, 150 mM NaCl, pH 7.4 at 37 °C over 12 days. The release medium was changed twice a day. Aliquots (20 μL) of each sample were withdrawn from the Float-A-Lyzer and diluted fifty times with 0.1% (*v*/v) Triton X-100 solution in Milli-Q water; after 10 min incubation at room temperature to disaggregate the lipoplexes, the Cy3-dsDNA concentration was measured by spectrofluorimetric analysis using an LS 50 B Perkin-Elmer fluorimeter (Waltham, MA, USA) with an excitation wavelength of 554 nm and emission of 568 nm. The concentration of Cy3-dsDNA in the samples was derived from a titration curve performed using dilutions of Cy3-dsDNA in 0.1% (v/v) Triton X-100 in Milli-Q water.

3.14. Gene knockdown studies

To study the ability of selected lipoplex formulations for functional siRNA delivery, two model tumor cell lines constitutively expressing luciferase transgene (namely MDA-MB-231-PGK-EGFP-Luc and HeLa-PGK-EGFP-Luc, as described above) were employed. These cells were treated with lipoplex formulations loaded at 10 N/P ratio with either Luc-siRNA (specific siRNA targeting luciferase mRNA) or NC-siRNA (sequence scrambled negative control siRNA) and subjected to firefly luciferase assay for quantifying luciferase enzyme expression. Cells were seeded into a white 96-well plate at a density of 10,000 cells/well for HeLa cell line and 20,000 cells/well for MDA-MB231 cell line, based on their growth differences. After 24 h from seeding, cells were treated with different lipoplex formulations at siRNA concentration of 50 nM (corresponding to 10 pmol siRNA per well). Cells were treated with lipoplexes loaded with either Luc-siRNA or NC-siRNA in HBS buffer. All lipoplex formulations were directly added in the complete cell culture medium i.e. with 10% serum and at same siRNA dosage of 10 pmol per well, based on picogreen assay quantification mentioned above. As positive control, cells were treated with lipofectamine at siRNA concentration of 5 nM (corresponding to 1 pmol Luc-siRNA or NC-siRNA per well), according to manufacturer's protocol. After 48 h of incubation with lipoplexes, media was discarded, and cells were washed with 200 μL of PBS and then lysed in 30 μL of passive lysis buffer (1× PLB per well) by incubation at room temperature under shaking at 500 rpm for 30 min. Out of the 30 μL cell lysate, 10 μL was used for firefly luciferase assay and 20 μL was analysed for protein amounts by bicinchoninic acid assay (BCA), as per the reported method [27]. siRNA knockdown for each lipoplex formulation is plotted as % RLU (relative light units) as described below:

$$\%RLU = \frac{RLU\ Luc\ siRNA\ lipoplexes}{RLU\ NC\ siRNA\ lipoplexes}$$

where RLU Luc siRNA lipoplexes is the RLU from cells treated with Luc-siRNA-lipoplexes and RLU NC siRNA lipoplexes is the RLU from cells treated with exactly same lipoplex formulation but loaded with NC-siRNA i.e. NC-siRNA-lipoplexes.

3.15. Endosomal escape kinetics studies

Endosomal escape kinetics of OCE-lipoplexes was indirectly investigated via knockdown of luciferase gene expression in presence or absence of lysosomotropic agent chloroquine, which destabilizes endosomal vesicles intracellularly [28]. MDA-MB-231-PGK-EGFP-Luc cells, constitutively expressing luciferase transgene, were used for studying the kinetics of endosomal escape of selected lipoplex formulations. Different conditions for chloroquine-treatment and lipoplex-uptake were investigated and include a) pre-treatment, b) co-treatment, c) pre-co treatment and d) post-treatment methods. For all treatment conditions, chloroquine was added at 100 μM and duration for chloroquine-treatment was 4 h, as this is the most routinely used treatment profile from a tolerable cytotoxicity standpoint. Pre-treatment method involved pre-incubation of the cells with chloroquine for 4 h and then media was changed before addition of lipoplexes for 44 h, followed by firefly luciferase assay. Pre-co-treatment method involved pre-incubation of cells with chloroquine for 1 h and then lipoplexes were added for 3 h (without medium change as in co-treatment with chloroquine), followed by media change and then firefly luciferase assay was performed 45 h later. In co-treatment method, both chloroquine and lipoplexes were added to cells for 4 h and then medium was changed, which was followed by an incubation step of 44 h and then firefly luciferase assay was performed. Within post-treatment method, first lipoplexes were added for different durations (12, 20 or 32 h) and then chloroquine was added for 4 h, followed by medium change and incubation for different durations so that firefly assay was performed 48 h after initial lipoplex addition.

Lipoplex formulations used for this study included lipoplexes based on either Luc-siRNA (specific siRNA targeting luciferase mRNA) or NC-siRNA (sequence scrambled negative control siRNA), as for the knockdown study described above and data was plotted similarly for percentage knockdown but as a function of presence or absence of chloroquine.

3.16. Statistical analysis

The data were expressed as mean ± SD calculated from at least three independent experiments. Statistical analysis was determined by the two-tailed Student's *t*-test using GraphPad 5 software.

4. Results and discussion

Cationic liposomes were obtained by introducing the oligo-cationic tetraArg-[G-1]-distearoyl glycerol (Arg_4-DAG) agent into the lipid bilayer. Arg_4-DAG was previously shown to promote the cell uptake of colloidal systems paving the way to its exploitation for delivery of nucleic acids [19,20]. According to its oligoarginine composition, Arg_4-DAG represents a bioinspired macromolecule that recapitulates the condensing features of the arginine-rich protein protamine, which is reported to efficiently condense and deliver nucleic acids while promoting their cell-uptake [29]. Additionally, cationic end tipped dendronic structures offer high surface charge density, which allow for efficient nucleic acid binding [30].

OCE decorated lipoplexes were prepared according to two strategies: (i) OCE inclusion in the lipidic mixture followed by lipid film hydration with water or aqueous solution of the nucleic acids to obtain OCE-LIP and OCE-LPX, respectively (Fig. 1A); (ii) OCE post-insertion on liposomes (OCE_{post}-LIP) followed by association with nucleic acids, OCE_{post}-LPX (Fig. 1B). In the first case (i, OCE-LPX), the nucleic acid was expected to be localized either inside the vesicle or on the surface, while in the second case (ii, OCE_{post}-LPX) the nucleic acid was expected to be only on the surface. OCE-free liposomes and lipoplexes (OCE_{free}-LIP and OCE_{free}-LPX, respectively) were prepared by film hydration and used as control. All formulations are summarized in Suppl. Fig. S7 and S8.

The OCE association to liposomes obtained by lipid film hydration with OCE included in the lipid film was preliminarily assessed in the absence of nucleic acids (OCE-LIP). The Sakaguchi assay [22] revealed that >90% of OCE was associated to liposomes formulated with 0–8 mol % OCE (OCE/lipids molar ratio) while association efficiency decreased to 75% with 10 mol% OCE. The liposome zeta potential was found to logarithmically increase with the OCE content (Suppl. Fig. S9A and S9C), from −0.6 ± 0.3 mV for 0 mol% OCE to +34.7 ± 2.1 mV for 10 mol% OCE liposomes, indicating that OCE inclusion slowly undergoes to saturation. OCE association was not found to alter the liposome size (176–192 nm) and the polydispersity (PdI < 0.1). The OCE post-insertion on preformed liposomes (OCE_{post}-LIP) yielded >90% of OCE association to liposomes formulated with 0–4 mol% OCE that decreased to 40% with 10 mol% OCE. Accordingly, the zeta potential was found to rapidly increase to reach a plateau of +28.1 ± 1.7 mV at 4 mol% OCE

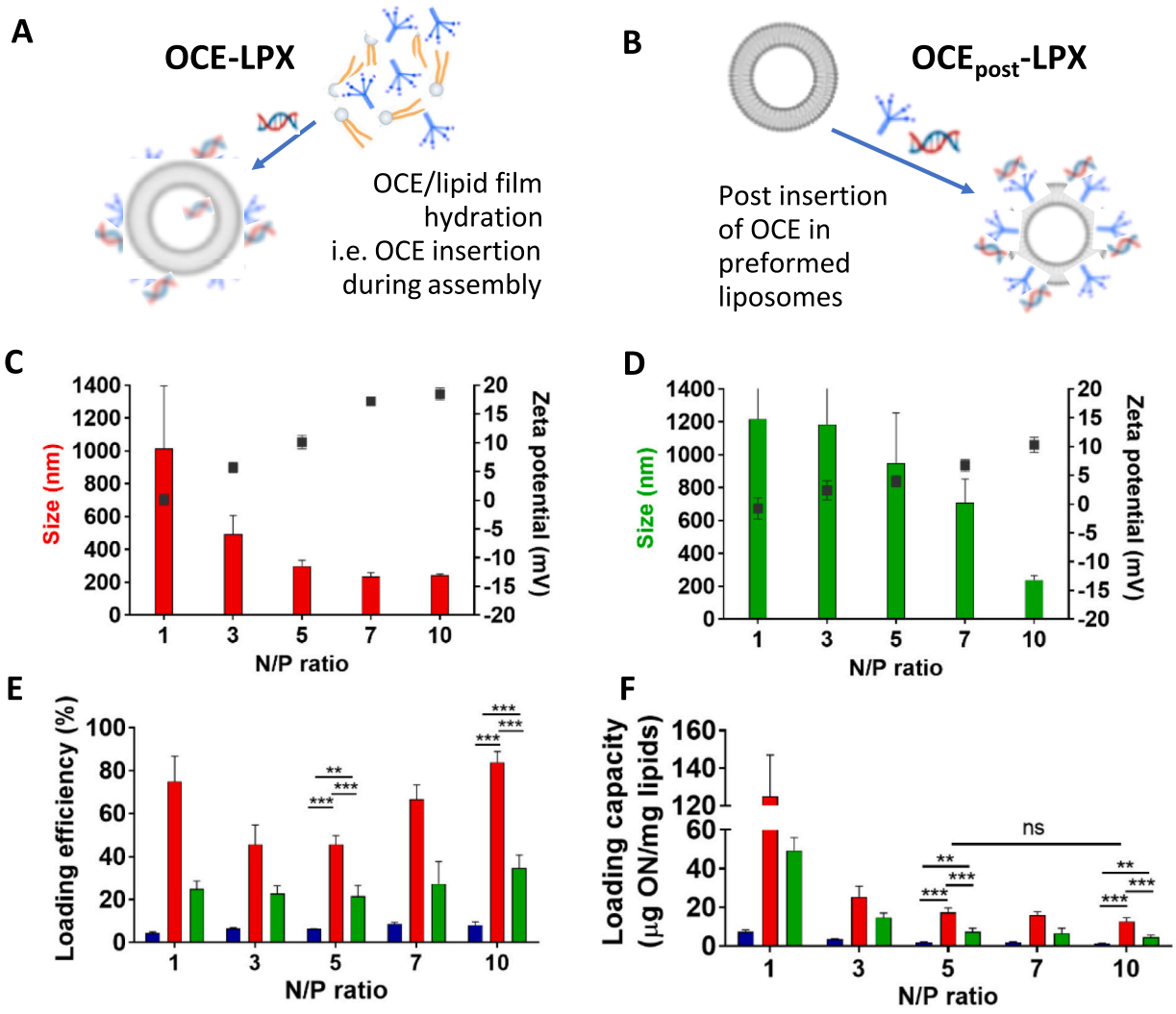

Fig. 1. Incorporation of non-peptidic oligocationic enhancer into liposomal nanocarrier for ON encapsulation.
Schematic representation of lipoplex assembly via two approaches: A) inclusion of oligocationic enhancer (OCE) within lipidic mixture followed by hydration with ON solution to get OCE-LPX lipoplexes and B) post-insertion of OCE on preformed liposomes followed by complexation with nucleic acids to get OCE$_{post}$-LPX lipoplexes. Size and zeta-potential characterization of OCE-LPX (C) and OCE$_{post}$-LPX (D) lipoplexes loaded with dsDNA at increasing N/P ratios. Loading efficiency (%; E), and loading capacity (*w*/w %; F) of OCE-LPX (■), OCE$_{post}$-LPX (■) and OCE$_{free}$-LPX (■) at increasing N/P ratios. Statistical analysis: ** $p < 0.01$; *** $p < 0.001$.

(Suppl. Fig. S9B and S9D). This result is consistent with the saturation of the liposome surface when OCE is post inserted to preformed liposomes. OCE-LIP and OCE$_{post}$-LIP showed similar size (177–188 nm) (Suppl. Fig. S9D).

OCE-LIP and OCE$_{post}$-LIP obtained with 4 mol% OCE that showed similar features were selected for comparative nucleic acid encapsulation evaluation (Fig. 1 A-B). Nucleic acid loaded lipoplexes (OCE-LPX and OCE$_{post}$-LPX) were prepared at different N/P ratios by employing two oligonucleotides (ONs), dsDNA and siRNA, with similar structure (double strand) and size (19 and 21 bp, respectively, and 11 and 13 kDa, respectively). The more stable dsDNA was used as model ON to set-up the formulation and select the system with suitable ON delivery properties. On the other hand, siRNA was used as bioactive model ON, to investigate the delivery and transfection efficiency of the selected lipoplexes.

Control OCE-free liposomes obtained by lipid film hydration yielded low ON loading regardless the ON feeds. Furthermore, size and zeta potential were not found to be affected by the ON feed (Suppl. Fig. S10).

In the case of OCE-LPX, the ON loading was found to affect both size and zeta-potential. Fig. 1C shows that the size increases significantly as the ON feed increases (N/P ratio decreases) suggesting that OCE-LPX undergo aggregation. This is probably due to the remarkable charge quenching (zeta potential decrease), which reaches near neutrality at 1 N/P. Low ON feeds (high N/P ratios) produce small OCE-LPX (233 and 243 nm with 7 and 10 N/P ratio, respectively) where the zeta potential (+17.3 and + 18.3 mV with 7 and 10 N/P ratio, respectively) is only slightly lower than that of OCE-LIP (+22.7 mV).

Fig. 1D shows that ON feed has stronger effect on size and of zeta potential OCE$_{post}$-LPX compared to OCE-LPX. OCE$_{post}$-LPX obtained with 10 N/P ratio yielded a zeta potential decrease of about 20 mV with respect to the OCE$_{post}$-LIP zeta potential.

The different effect of ON feed on zeta potential of the formulations obtained with the two OCE insertion procedures is ascribable to the different OCE localization in OCE-LPX and OCE$_{post}$-LPX. Indeed, although OCE-LPX and OCE$_{post}$-LPX obtained with 4 mol% OCE possess similar OCE/lipid molar ratio, in OCE-LPX the OCE is partially distributed in the internal compartment of liposomes while in OCE$_{post}$-LPX OCE is distributed only on the vesicle surface. When same ON feed is used to produce the two formulations, ON is only associated to the OCE$_{post}$-LPX surface while in the case of OCE-LPX prepared by film

hydration, it is partially distributed in the liposome core.

The results summarized in Fig. 1E and F show that OCE-LPX possess significantly higher loading efficiency and capacity in comparison to OCE_{free}-LPX counterparts at all N/P ratios. Interestingly, also OCE_{post}-LPX showed higher loading efficiency and capacity than OCE_{free}-LPX, although the latter were prepared by film hydration that incorporates the ON in hydrating solution. Furthermore, as expected, except OCE-LPX and OCE_{post}-LPX obtained at 1 N/P ratio that were found to undergo aggregation, the loading efficiency of OCE-LPX increased as the ON feed decreased (N/P ratio increased). These results all together indicate that OCE has a remarkable ability to associate with ONs.

The thermodynamic contribution to the OCE/ON interaction (Suppl. Fig. S11) was investigated by isothermal microcalorimetric titration of OCE_{post}-LIP and OCE_{free}-LIP with ONs. OCE_{post}-LIP were used to guarantee the complete access of the ON to OCE associated onto the liposomes.

Isothermal microcalorimetry did not show interactions between OCE_{free}-LIP and ON (Suppl. Fig. S12), while OCE_{post}-LIP titration with ON showed an exothermic profile fitting one binding site behavior. The association was found to occur by an enthalpy-driven process ($\Delta H = -11.8 \pm 0.4*10^4$ cal/mol) with entropy decrease ($\Delta S = -361$ cal/mol*K) resulting in a strong association constant (K_a, $4.03 \pm 1.03*10^7$ M^{-1}) (Suppl. Fig. S11A). It should be noted that the association parameters are similar to those obtained with other cationic liposomes reported in the literature [31–34].

The calorimetric titration profiles obtained in 10 mM HEPES and in 10 mM HEPES/NaCl (0.15 and 0.3 M NaCl) showed that the OCE/ON association decreases as the ionic force increases (Suppl. Fig. S11 B—D). In the presence of 0.3 M NaCl, the OCE_{post}-LIP/ON calorimetric profile (Suppl. Fig. S11D) almost overlapped the ones of the OCE_{free}-LIP/ON (Suppl. Fig. S11 *E*-G). At physiological ionic strength of 0.15 M NaCl (Suppl. Fig. S11 C), the OCE/ON K_a is $1.78 \pm 0.29*10^7$ M^{-1}, which is 2.3 times lower than the K_a measured in Milli-Q water. These results indicate that the OCE/ON association is dictated by ionic interactions.

Heparin displacement studies were performed by gel electrophoresis to further investigate the OCE/ON association stability under physiological conditions. OCE_{free}-LPX yielded bands corresponding to free ON at all tested heparin concentrations (Suppl. Fig. S13 A). On the contrary, gel electrophoresis of OCE-LPX did not show bands corresponding to free ON up to 6 IU/mL heparin incubation (Suppl. Fig. S13 B) indicating that at physiological heparin concentration (0.15 IU/mL) ON is associated to OCE [35].

According to the ON loading results reported above, 5 and 10 N/P ratio OCE-LPX were selected as the best candidates for ON delivery. However, in physiological buffer at 37 °C, 5 N/P ratio OCE-LPX was found to undergo aggregation in few hours (Suppl. Fig. S14) while 10 N/P OCE-LPX were stable over 7 days. Therefore, 10 N/P OCE-LPX were selected for further studies.

Aimed at investigating the effect of PEG on biopharmaceutical and transfection properties of OCE decorated lipoplexes, OCE-LPX and OCE_{free}-LPX were decorated with PEG by post-insertion of PEG_{2kDa}-DSPE or PEG_{5kDa}-DSPE at increasing PEG-DSPE/lipid ratios to obtain PEG-OCE-LPX. Lipoplexes were loaded at 10 N/P dsDNA or siRNA (scrambled siRNA and Luc-siRNA) as models for comparison with previous data and for biological investigations.

Dynamic light scattering (DLS) analysis reported in Fig. 2A-B show

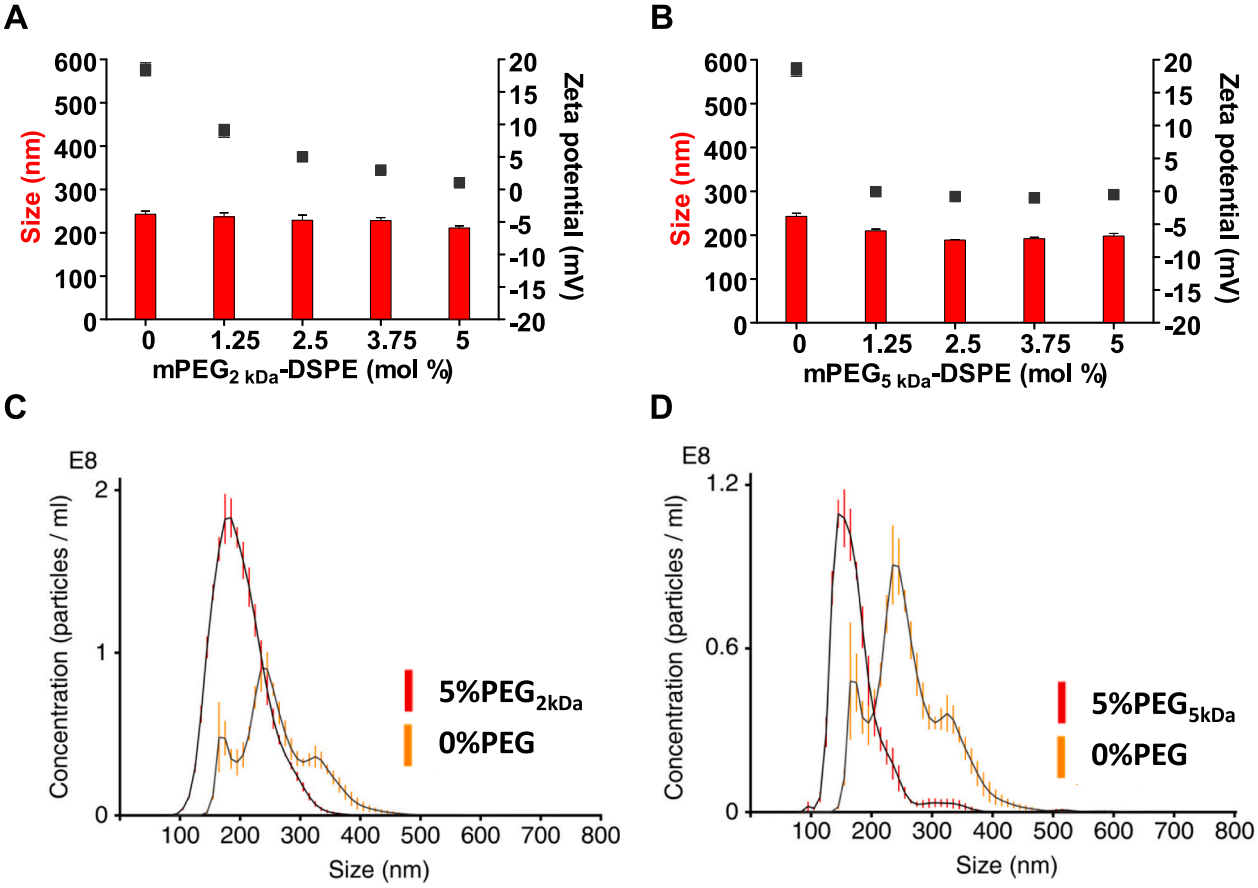

Fig. 2. Comprehensive characterization of PEGylated ON loaded oligo-cationic enhancer functionalized lipoplexes (OCE-LPX) by light scattering techniques. Dynamic light scattering-based size (■) and Zeta potential (■) of dsDNA loaded OCE-LPX at 10 N/P ratio and decorated with increasing mol % of $mPEG_{2kDa}$-DSPE (A) or $mPEG_{5kDa}$-DSPE (B). NTA-based size population distribution of OCE-LPX at 10 N/P ratio without and with 5 mol% of $mPEG_{2kDa}$-DSPE (C) or $mPEG_{5kDa}$-DSPE (D) coating.

that, as expected, the zeta potential of PEG-OCE-LPX formulations decreased as the molecular weight of PEG and the PEG-DSPE/lipid molar ratio increased while control OCE_{free}-LPX showed no change in zeta potential and size upon PEGylation (Suppl. Fig. S15). Nearly neutral surfaces of PEG-OCE-LPX were obtained with 5 mol% PEG_{2kDa} (+ 2 mV) and 1.25 mol% PEG_{5kDa} (−1 mV). High surface density PEG_{2kDa} (5 mol% PEG_{2kDa}) decoration yielded slight size decrease while slight size decrease was observed also with low surface PEG_{5kDa} density (1.25 mol % PEG_{5kDa}), which is in agreement with observations reported in the literature [36]. The nanoparticle tracking analysis (NTA) reported in Fig. 2C-D shows that both PEG_{2kDa} and PEG_{5kDa} coated OCE-LPX have narrower size distribution than the non-PEGylated counterparts. The 2D plots of scattering-intensity vs size (Suppl. Figs. S16) confirmed that the whole nanoparticle size population shifts to smaller size after post-insertion PEGylation. Also, here the effect of PEG_{5kDa} seems to shift the nanoparticle population towards smaller distribution (Suppl. Fig. S16B), in comparison to PEG_{2kDa} (Suppl. Fig. S16A).

We also tested lipoplexes loaded with biologically active siRNA. Hence, first we optimized a precise quantification of siRNA by using picogreen dye for preparing calibration lines with Luc-siRNA and the negative-control scrambled siRNA (Suppl. Fig. S17 A-D) and also tested if any interference from Triton-X used to disassemble lipoplexes before siRNA-quantification occurs (Suppl. Fig. S17 E-F). Both Luc-siRNA (Suppl. Fig. S17-A, S17—C) and scrambled siRNA (Suppl. Fig. S17—B, S17—D) showed a very good linear correlation of siRNA estimation at increasing concentration. Indeed, Triton-X interfered slightly with siRNA estimation (Suppl. Fig. S17 E-F). Thus, optimized picogreen assay with Triton-X was employed to reliably quantify siRNA load in lipoplex formulations as a function of OCE and PEGylation (Suppl. Fig. S18). The ON loading in PEGylated and non-PEGylated OCE-LPX and OCE_{free}-LPX was determined by picogreen using Luc-siRNA loaded polyplexes. The results showed that neither capacity nor efficiency were affected by the PEG molecular weight and coating density (Suppl. Fig. S18) indicating that the PEG post insertion neither displaced the ON associated on the lipoplex surface nor induced lipoplex leaking and ON release.

DLS analyses were carried out to evaluate the protein association to PEGylated OCE-LPX when incubated with 10% FBS medium. Fig. 3 reports the lipoplex size after 8 h incubation. OCE_{free}-LPX were found to be stable either in buffer or in FBS medium, while OCE-LPX were stable in protein free buffer medium but underwent rapid and remarkable size increase (>1 μm) in FBS medium forming large aggregates at 8 h of incubation and beyond. Although 2.5 and 5% PEG_{2kDa} coating was found to prevent the formation of large aggregates in FBS medium, some size enlargement (~400 nm) was observed at 8 h, whereas no further size increase was observed at 24 h of incubation. With PEG_{5kDa} coating of OCE-LPX less size increase was observed at both mol % pointing at a better shielding effect.

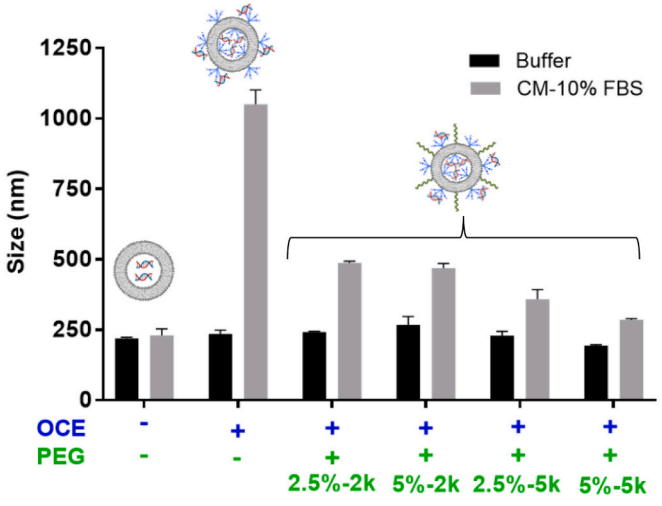

Fig. 3. PEGylation negates serum-induced increase in hydrodynamic diameter of lipoplexes.
DLS based hydrodynamic diameter of dsDNA loaded lipoplexes at 10 N/P ratio: OCE_{free}-LPX and OCE-LPX without PEG, OCE-LPX/PEG_{2kDa} with 2.5 or 5 mol% PEG_{2kDa}, OCE-LPX/PEG_{5kDa} with 2.5 or 5 mol% of PEG_{5kDa}, when incubated for 8 h in either complete DMEM with 10% FBS (CM-10%FBS) or 10 mM HEPES, 150 mM NaCl pH 7.4 buffer (HBS) at 37 °C.

The stability of the best performing formulation, PEG_{5kDa} coated OCE-LPX, was tested in whole rat plasma. The electrophoresis analysis of samples incubated with rat plasma at different times did not show bands corresponding to the ON indicating that ON was stably associated into the lipoplexes (Suppl. Fig. S19 A). The electrophoresis of samples obtained by lipoplex co-incubation with rat plasma and heparin as positive control yielded the ON bands with increasing intensity over 24 h incubation indicating that ON was released from the lipoplexes (Suppl. Fig. S19 B).

The lipoplex cytotoxicity was determined by incubation with MDA-MB-231 cells. Fig. 4A shows that PEGylated and non-PEGylated OCE_{free}-LPX do not affect cell viability. Fig. 4B shows that the cell viability assessed by incubation with all tested doses of non-PEGylated and 2.5 mol% PEG_{2kDa} coated OCE-LPX was lower than that of OCE-free counterparts, while OCE-LPX coated with 5 mol% PEG_{2kDa}, 2.5 and 5 mol% PEG_{5kDa} did not elicit significant cytotoxicity even at high doses.

Fig. 5 reports the hemolytic behavior of 10 N/P ON loaded lipoplexes. All formulations under the tested conditions showed low hemolytic activity even at high doses (≤5%) with respect to control samples (Suppl. Fig. S20) indicating that neither OCE nor PEG had a negative effect on lipoplex biocompatibility.

Flow cytometry and confocal microscopy studies were carried out to investigate the effect of PEG and OCE on cell interaction and uptake of lipoplexes. Majzoub et al. [37] reported in fact that PEGylation reduces the cell penetration of a variety of cationic nanoparticles, while OCE was found to enhance the cell interaction and up-take of nanovesicles [20]. The studies were performed by incubating HeLa and MDA-MB-231 cells for 1 h and 24 h with 10 N/P fluorescent AF-647 labelled ON loaded lipoplexes.

The cytofluorimetric profiles reported in Fig. 6 (Suppl. Fig. S21) show that after 1 h incubation with HeLa cells yielded little percentage of OCE_{free}-LPX associated cells while after 24 h incubation showed an increased number of lipoplexes associated cells, which was only slightly affected by the PEG coating.The histogram plots and MFI profiles (Suppl. Fig. S21 and S22, respectively) show lower overall lipoplex association at 24 h incubation for all OCE_{free}-LPX samples (PEGylated and non-PEGylated lipoplexes), in comparison to the OCE-LPX counterparts. After 1 h incubation, the OCE-LPX associated at higher percentage and extent with HeLa cells with respect to the OCE_{free}-LPX and the cell interaction of the former was found to be affected by the PEG coating (Fig. 6). After 1 h incubation the MFI data (Suppl. Fig. S22) show that the extent of association of OCE-LPX coated with 5 kDa PEG was more than double than the one of non-PEGylated and 2 kDa PEG coated formulations. The higher association of PEGylated OCE-LPX with respect to the non-PEGylated counterparts may be ascribed to the higher colloidal stability of the former in the presence of serum. To note that the cytofluorimetric data (Fig. 6 and Fig. S21) show that after 24 h incubation the differences among PEGylated OCE-LPX are less relevant, indicating that the PEG composition on the lipoplex surface strongly affects the association kinetics rather than the overall association.

The results obtained by incubation of OCE-LPX with MDA-MB-231 and HeLa cells reported in Fig. 6 (Suppl. Fig. S23 and S24) show similar association behaviors. OCE_{free}-LPX underwent much lower cell association compared to the OCE-LPX. The higher OCE_{free}-LPX association obtained with HeLa cells at 24 h with respect to MDA-MB-231 cells may be due to surface differences of cell membranes and differences in endocytic profiles, as also observed by other studies [38,39]. The zeta potential of HeLa and MDA.MB-231 cells are −13 mV [40] and − 25 mV

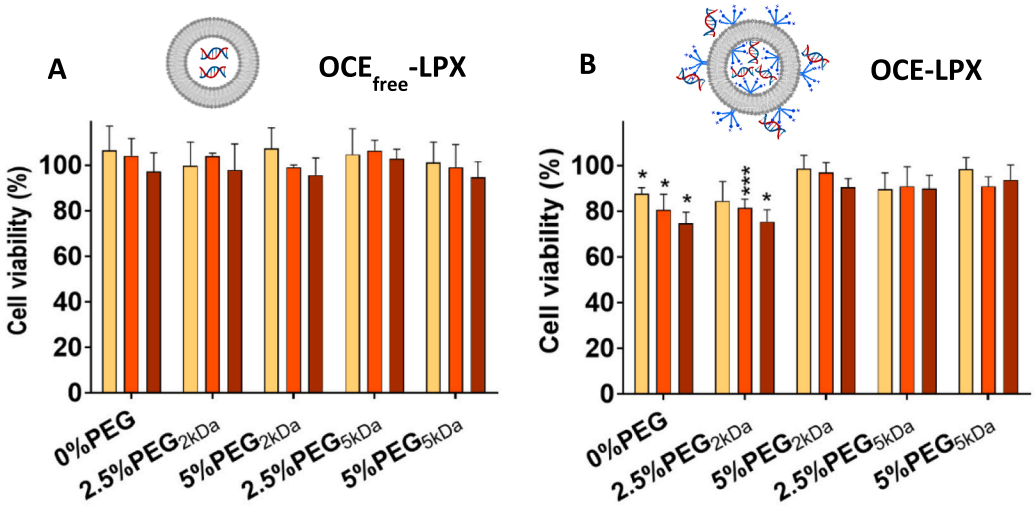

Fig. 4. Effect of oligocationic enhancer and PEGylation on cell viability profile.
MTT assay-based viability of MDA-MB-231 cells incubated for 24 h with lipoplexes loaded at 10 N/P ratio: OCE_{free}-LPX (A) and OCE-LPX (B) decorated with different molar ratio and different molecular weight of PEG. Liposomal formulations were tested at treatment concentrations of 50 (■), 125 (■) and 250 (■) nM of dsDNA. Statistical analysis versus the equimolar OCE_{free}-LPX formulation: * $p < 0.05$; *** $p < 0.005$.

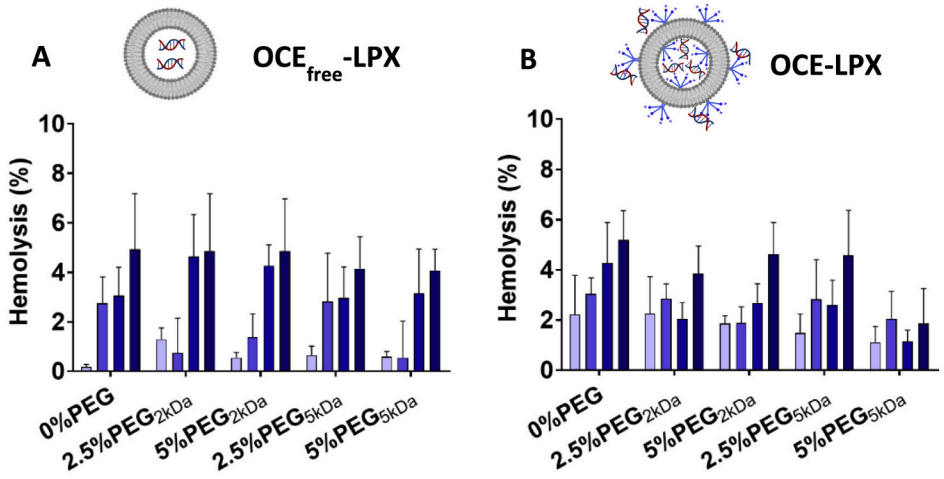

Fig. 5. Effect of oligocationic enhancer and PEGylation on lipoplex induced hemolysis.
Hemolytic profiles of dsDNA loaded lipoplexes at 10 N/P ratio based on OCE_{free}-LPX (A) and OCE-LPX (B) decorated with PEG at different molar ratio and different molecular weight. Lipoplex formulations were tested at treatment concentrations of 0.05 (■), 0.1 (■), 0.2 (■) and 0.3 (■) mg/mL of lipids.

[41], respectively while the OCE_{free}-LPX zeta potential is −2.5 mV. Therefore, lower electrostatic repulsion are expected to take place between OCE_{free}-LPX and HeLa cells with respect to OCE_{free}-LPX and MDA-MB-231 resulting in higher OCE_{free}-LPX association to HeLa cells with respect to MDA-MB-231 in the long time incubation.

The confocal microscopy images reported in Fig. 7 show that neither PEGylated nor non-PEGylated OCE_{free}-LPX are internalized after 1 h incubation with MDA-MB-231 cells. In contrast, both PEGylated and non-PEGylated OCE-LPX show visible fluorescent red spots in the cytosol. Similar results have been obtained with AF647-siRNA or Cy3-dsDNA loaded lipoplexes (Suppl. Fig. S25). The magnified images reported in Fig. 7E and F show large intracellular spots of non-PEGylated and PEGylated OCE-LPX, indicating successful intracellular delivery of siRNA via the OCE functionalization and even in presence of 5% PEG. It is noteworthy that 5% PEG_{5kDa} leads to considerable stability in serum but also allows successful intracellular siRNA delivery because of the presence of OCE.

According to the evidence that the OCE_{free}-LPX were not efficiently taken up by cells, the lipoplex ability to release and deliver biologically active ONs was carried out with OCE-LPX and PEGylated OCE-LPX using Cy3-dsDNA and Luc-siRNA loaded lipoplexes, respectively.

Release studies showed that the ON is released slowly in several days from non-PEGylated and PEGylated lipoplexes (Fig. 8). In both cases, the release takes place according to a bimodal behavior: a faster release of about 25% of loaded ON in the first 8 h followed by very slow release of about 60% in 6 days. The initial faster release can be due to ON fraction associated to the lipoplex surface. The presence of either 2 kDa or 5 kDa PEG on lipoplexes surface had a limited impact on the ON release showing that it does not interfere with the association of the ON to the lipoplexes over time..

The siRNA delivery was investigated by using Luc-siRNA loaded lipoplexes and three cancer cell types constitutively expressing the luciferase reporter gene: Hela-PGK-EGFP-Luc, MCF7-PGK-EGFP-Luc and MDA-MB-231-PGK-EGFP-Luc. Scrambled-siRNA loaded formulations

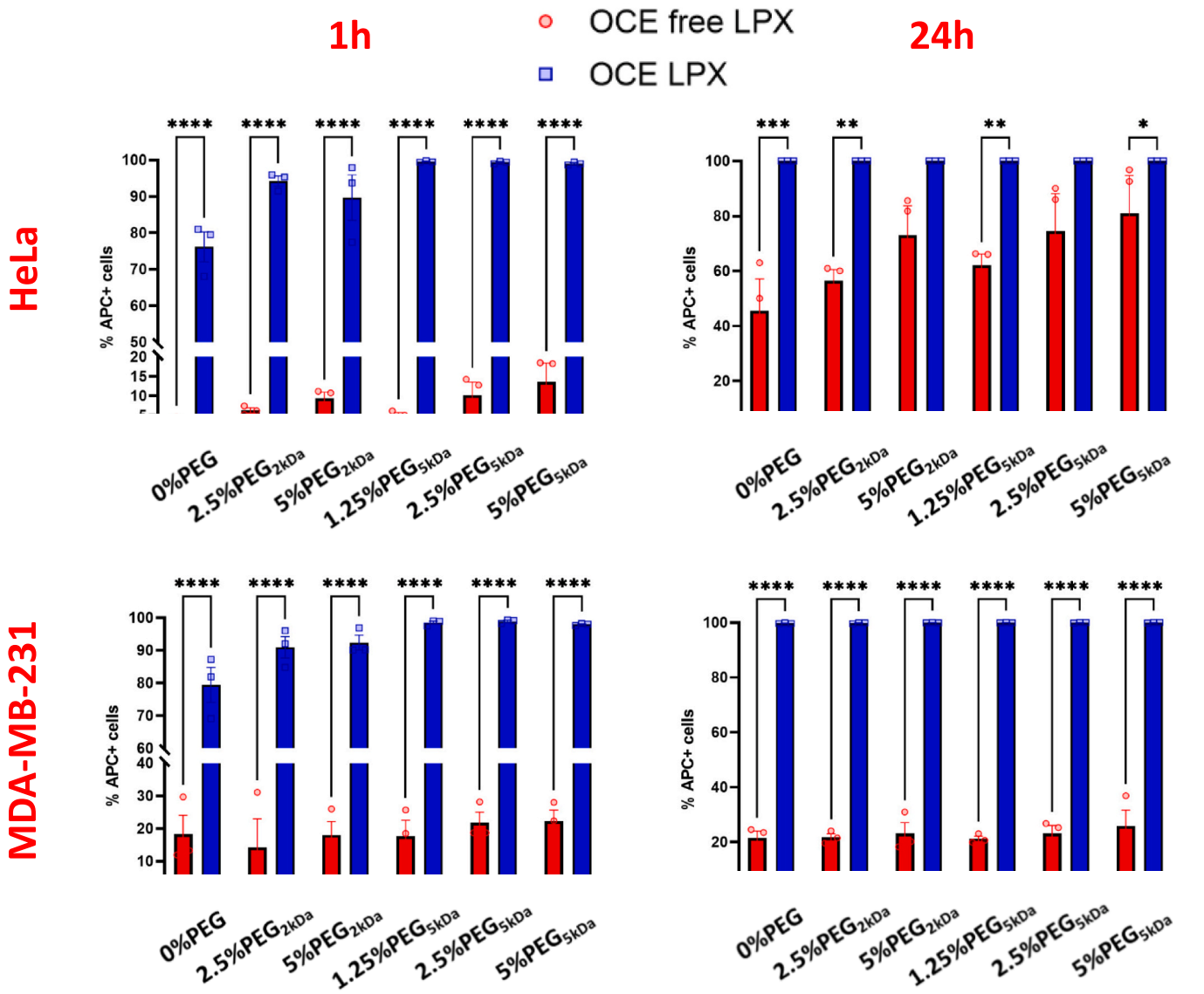

Fig. 6. Effect of oligocationic enhancer and PEGylation on cell association of lipoplexes to cancer cells.
Percentage of positive cells for AF647 fluorescence signal after HeLa and MDA-MB-231 cells were treated for 1 h or 24 h with lipoplexes loaded with AF647-siRNA at 10 N/P ratio: OCE_{free}-LPX (red bars) and OCE-LPX (blue bars) decorated with PEG at different ratio and different molecular weight. Data were analysed with *t*-test statistics, $p < 0.05$ (*); $p < 0.01$ (**); $p < 0.001$ (***); $p < 0.0001$ (****). Data shown is average of three experiments, with each experiment including 10,000 single cell events: mean ± SD.

were used as negative control while Luc-siRNA loaded lipofectamine formulations were used as positive control. The transfection data reported in Suppl. Fig. S26 show that the tested lipoplex formulations did not display silencing effect on the breast cancer cell lines MCF-7 and MDA-MB-231 cells, while in HeLa cells, some luciferase gene expression inhibition was found when treated with PEG_{5kDa}-OCE-LPX. Actually, it is well known that cell lines have different endocytic profile including differences in endocytic uptake, *endo*-lysosomal localization, trafficking and recycling, which affects the intracellular fate of colloidal drug delivery systems and their therapeutic outcome [38]. The knockdown activity results suggests that the PEG on the lipoplex surface could play some role in favoring the ON escape from lysosomes, which seems to depend on a combination of PEG density and molecular weight. This aspect may be of particular relevance in designing efficient lipoplexes and additional sophisticated studies must be performed to elucidate the role of PEG in the transfection process. Although with PEGylated lipoplexes some knockdown can be achieved, the overall performance is low, despite the very efficient uptake (see above). The oligo-arginine like structure in the OCE headgroup has similarities with certain arginine-rich peptides termed cell penetrating peptides (CPP). Like CPPs, OCE-LPX are very efficiently internalized by cells, with or without PEGylation, but both have shortcomings in endosomal release [42]. In order to pinpoint the reasons for the lack of target knockdown and if hampered endosomal release is indeed the main bottleneck, studies were carried out by using chloroquine, a known lysosomotropic agent with the ability to buffer endosomal vesicles thus promoting the endosomal escape of nanocarriers induced by osmotic effects [18,28,43]. Within preliminary studies carried out to set-up the experimental conditions to evaluate the transfection efficiency of OCE-lipoplexes in the presence of chloroquine, pre- and co-incubation with chloroquine did not induce any knockdown activity (data not shown). This can be at least in part explained by the fact that chloroquine negatively interferes with clathrin

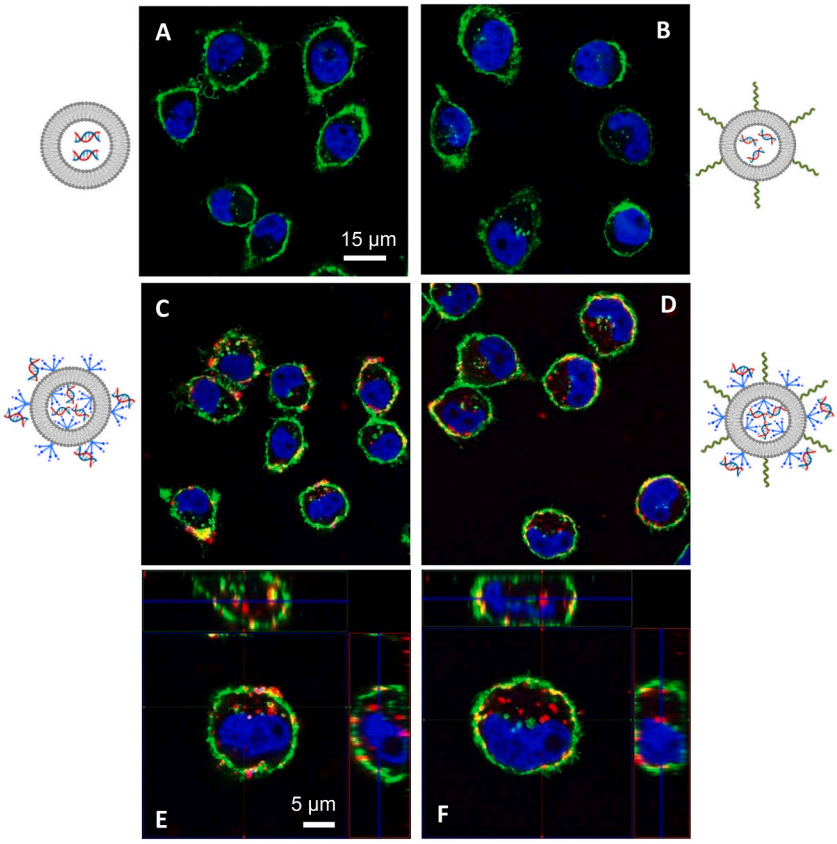

Fig. 7. Intracellular localization of fluorescently-labelled formulations in MDA-MB-231 cells.
Confocal microscopy images of MDA-MB-231 cells incubated for 1 h with AF647-siRNA (red) loaded lipoplexes (10 N/P ratio). OCE_{free}-LPX (A), OCE_{free}-LPX with 5 mol% PEG_{5kDa} (B), OCE-LPX (C), OCE-LPX with 5 mol% of PEG_{5kDa} (D). Magnification of the white squares of panel C and D are reported in panels E and F (with *Z*-projections), respectively. Cell nuclei were stained with DAPI (blue) and cell membranes with WGA-AlexaFluor 488 (green).

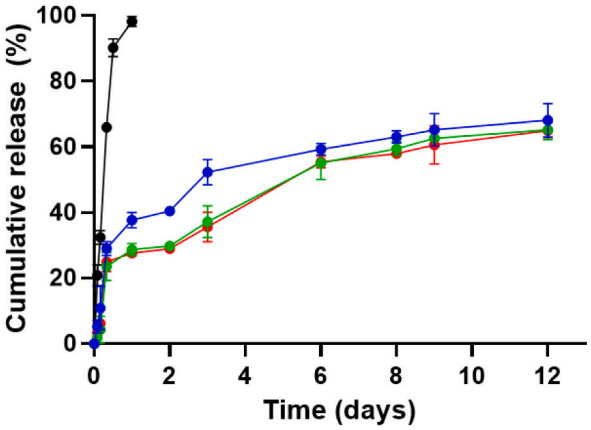

Fig. 8. Release of fluorescently-labelled ON from lipoplexes.
Release of Cy3-dsDNA from OCE-LPX (●), 5 mol% PEG_{2kDa} coated OCE-LPX (●) and 5 mol% PEG_{5kDa} coated OCE-LPX (●) in 10 mM HEPES, 150 mM NaCl, pH 7.4 at 37 °C. Diffusion profile of non formulated Cy3-dsDNA (●) through dialysis membrane under the same conditions.

mediated endocytosis [44] (reviewed in [45]), thereby negatively affecting lipoplex uptake. Hence, we applied a post-treatment strategy, ensuring that liposomes are already internalized at the onset of chloroquine treatment.

Surprisingly, both OCE-LPX and PEGylated OCE-LPX showed significant reduction of the luciferase signal by 50–60% when cells were incubated with lipoplexes for 12 or 20 h and a subsequent chloroquine treatment for 4 h (Fig. 9A-B). This shows that there is still functional siRNA present in the endolysosomal compartment for 12–20 h, which is then released to the cytoplasm due to the endosomolytic activity of the drug [28]. Thus, it is available for the knockdown machinery as evident by the specific reduction of luciferase activity. Apparently, OCE-LPX can protect siRNA from lysosomal degradation during this 12–20 h time window, also in the presence of PEG. This is also supported by data showing OCE-LPX and PEGylated OCE-LPX are already inside the cells after one hour of incubation and remain there (Fig. 7 and Fig. 6). In a related study, we could demonstrate protection of plasmid DNA inside lysosomes for at least 12 h by using the polycation linear polyethylenimine (LPEI). Here we treated cells with a photosensitizer, which after membrane association and subsequent activation by a laser pulse enabled triggered release of nucleic acid payload from intracellular vesicles [46]. For our LPX study we have employed a chemically stabilized Luc-siRNA with two phosphorothioate bonds on the 3′ terminus of the sense strand and one 3′ terminal phosphorothioate bond on the antisense strand [47]. This can additionally slow down degradation by exonucleases [48]. On the other hand, after a 32 h incubation period with lipoplexes and subsequent chloroquine treatment, a reduction in luciferase signal was not observed (Fig. 9C). This indicates at a possible siRNA degradation after this extended period of incubation with lipoplexes.

Endosomal processing times are crucial for successful nucleic acid delivery: Sayers and colleagues have identified a rather narrow time window for endosomal release before lysosomal degradation [49]. In our present work we identify the residence time of lipoplexes containing stabilized siRNA in the *endo*-lysosomal compartment. With this

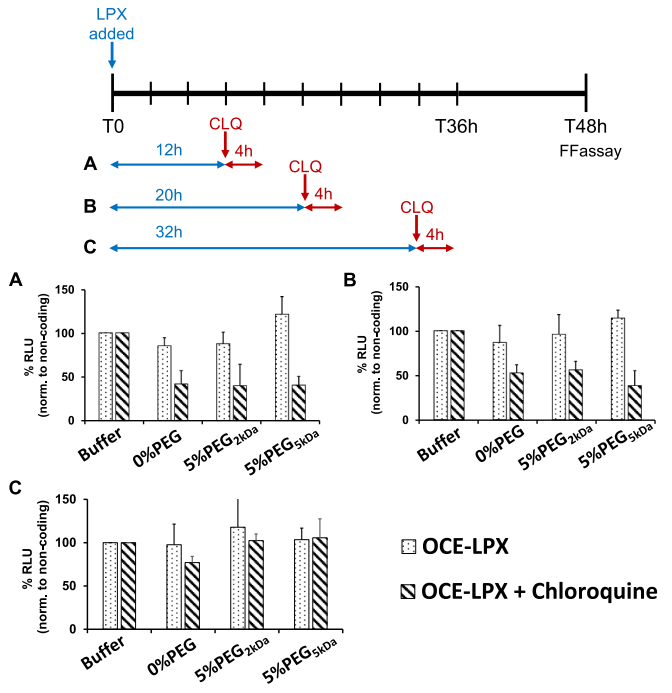

Fig. 9. Endosomal escape kinetics study: gene knockdown of OCE-LPX formulations in absence or presence of lysosomotropic agent after different extent of cell uptake of lipoplexes.
MDA-MB-231-PGK-EGFP-Luc cells were incubated with Luc-siRNA or NC-siRNA loaded OCE-LPX formulations prepared at N/P ratio 10 for A) 12 h, B) 20 h C) 32 h followed by 4 h-chloroquine treatment. Data shown is average of two-three independent experiments: mean ± SD.

knowledge, approaches can be designed where extracellular, physical stimuli can be applied for timely activation [46,50].

5. Conclusions

Taken together, we present here a liposomal delivery platform for nucleic acid-based drugs representing high loading capacity, biocompatibility and cellular delivery efficiency. By combining an OCE with permanent cationic charge and optimized PEG-lipid coating, cellular uptake could be maximized. With the lysosomotropic drug chloroquine endosomal release was unambiguously identified as a bottleneck, but also demonstrating that OCE-LPX can efficiently protect siRNA from degradation.

CRediT authorship contribution statement

Alessio Malfanti: Formal analysis, Investigation, Validation. **Haider Sami:** Formal analysis, Methodology, Supervision, Visualization, Data curation, Writing – original draft. **Anna Balasso:** Investigation, Visualization, Formal analysis, Writing – original draft. **Giulia Marostica:** Investigation. **Busra Arpac:** Formal analysis, Validation, Software, Visualization. **Francesca Mastrotto:** Data curation, Formal analysis, Methodology, Validation. **Giuseppe Mantovani:** Methodology, Resources. **Elisa Cola:** Investigation. **Martina Anton:** Resources, Validation. **Paolo Caliceti:** Funding acquisition, Resources, Writing – review & editing. **Manfred Ogris:** Resources, Supervision, Writing – review & editing, Funding acquisition. **Stefano Salmaso:** Conceptualization, Supervision, Writing – review & editing, Funding acquisition, Project administration, Resources.

Declaration of Competing Interest

None.

Data availability

Data will be made available on request.

Acknowledgements

This research was supported by EU funding within the MUR PNRR "National Center for Gene Therapy and Drugs based on RNA Technology" (Project no. CN00000041 CN3 Spoke #6 "RNA chemistry", Spoke #8 "Platforms for RNA/DNA delivery").

We are grateful to Prof Franz Gabor and Maria Anzengruber (Division for Pharmaceutical Technology, Department of Pharmaceutical Sciences) for giving access to the DLS measurements.

Appendix A. Supplementary data

Supplementary data to this article can be found online at https://doi.org/10.1016/j.jconrel.2023.09.022.

References

[1] K.E. Lundin, O. Gissberg, C.I. Smith, Oligonucleotide therapies: the past and the present, Hum. Gene Ther. 26 (2015) 475–485.
[2] H. Xiong, R.N. Veedu, S.D. Diermeier, Recent advances in oligonucleotide therapeutics in oncology, Int. J. Mol. Sci. 22 (2021).
[3] S. Thakur, A. Sinhari, P. Jain, H.R. Jadhav, A perspective on oligonucleotide therapy: approaches to patient customization, Front. Pharmacol. 13 (2022).
[4] J. Wan, J.A. Bauman, M.A. Graziewicz, P. Sazani, R. Kole, Oligonucleotide therapeutics in cancer, Cancer Treat. Res. 158 (2013) 213–233.
[5] R.L. Juliano, The delivery of therapeutic oligonucleotides, Nucleic Acids Res. 44 (2016) 6518–6548.
[6] A.E. Labatut, G. Mattheolabakis, Non-viral based miR delivery and recent developments, Eur. J. Pharm. Biopharm. 128 (2018) 82–90.
[7] C. Liu, L. Zhang, W. Zhu, R. Guo, H. Sun, X. Chen, N. Deng, Barriers and strategies of cationic liposomes for Cancer gene therapy, Mol. Ther. Meth. Clin. Dev. 18 (2020) 751–764.
[8] M. Rezaee, R.K. Oskuee, H. Nassirli, B. Malaekeh-Nikouei, Progress in the development of lipopolyplexes as efficient non-viral gene delivery systems, J. Control. Release 236 (2016) 1–14.
[9] P.A. Wender, D.J. Mitchell, K. Pattabiraman, E.T. Pelkey, L. Steinman, J. B. Rothbard, The design, synthesis, and evaluation of molecules that enable or enhance cellular uptake: peptoid molecular transporters, Proc. Natl. Acad. Sci. 97 (2000) 13003–13008.
[10] P.A. Wender, E. Kreider, E.T. Pelkey, J. Rothbard, C.L. VanDeusen, Dendrimeric molecular transporters: synthesis and evaluation of tunable polyguanidino dendrimers that facilitate cellular uptake, Org. Lett. 7 (2005) 4815–4818.
[11] L. Albertazzi, M. Serresi, A. Albanese, F. Beltram, Dendrimer internalization and intracellular trafficking in living cells, Mol. Pharm. 7 (2010) 680–688.
[12] D. Kalafatovic, E. Giralt, Cell-penetrating peptides: design strategies beyond primary structure and amphipathicity, Molecules 22 (2017) 1929.
[13] S.L.Y. Teo, J.J. Rennick, D. Yuen, H. Al-Wassiti, A.P.R. Johnston, C.W. Pouton, Unravelling cytosolic delivery of cell penetrating peptides with a quantitative endosomal escape assay, Nat. Commun. 12 (2021) 3721.
[14] A. Erazo-Oliveras, N. Muthukrishnan, R. Baker, T.-Y. Wang, J.-P. Pellois, Improving the endosomal escape of cell-penetrating peptides and their cargos: strategies and challenges, Pharmaceuticals 5 (2012) 1177–1209.
[15] H.Y. Xue, S. Liu, H.L. Wong, Nanotoxicity: a key obstacle to clinical translation of siRNA-based nanomedicine, Nanomedicine (London) 9 (2014) 295–312.
[16] Y. Xia, J. Tian, X. Chen, Effect of surface properties on liposomal siRNA delivery, Biomaterials 79 (2016) 56–68.
[17] G. McClorey, S. Banerjee, Cell-penetrating peptides to enhance delivery of oligonucleotide-based therapeutics, Biomedicines 6 (2018).
[18] H. Du Rietz, H. Hedlund, S. Wilhelmson, P. Nordenfelt, A. Wittrup, Imaging small molecule-induced endosomal escape of siRNA, Nat. Commun. 11 (2020) 1809.
[19] H. Popilski, V. Feinshtein, S. Kleiman, A. Mattarei, M. Garofalo, S. Salmaso, D. Stepensky, Doxorubicin liposomes cell penetration enhancement and its potential drawbacks for the tumor targeting efficiency, Int. J. Pharm. 592 (2021) 120012.
[20] M. Barattin, A. Mattarei, A. Balasso, C. Paradisi, L. Cantù, E. Del Favero, T. Viitala, F. Mastrotto, P. Caliceti, S. Salmaso, pH-controlled liposomes for enhanced cell penetration in tumor environment, ACS Appl. Mater. Interfaces 10 (2018) 17646–17661.
[21] A.D. Bangham, M.M. Standish, J.C. Watkins, Diffusion of univalent ions across the lamellae of swollen phospholipids, J. Mol. Biol. 13 (1965) 238–252.
[22] S. Sakaguchi, Über die katalytische wirkung des blutfarb-stoffes auf natriumhypochlorit nebst einer neuen farbenreaktion des blutes, J. Biochem. 5 (1925) 13–24.
[23] G.E.C. Sims, T.J. Snape, A method for the estimation of polyethylene glycol in plasma protein fractions, Anal. Biochem. 107 (1980) 60–63.

[24] J.C.M. Stewart, Colorimetric determination of phospholipids with ammonium ferrothiocyanate, Anal. Biochem. 104 (1980) 10–14.
[25] A. Taschauer, A. Geyer, S. Gehrig, J. Maier, H. Sami, M. Ogris, Up-scaled synthesis and characterization of nonviral gene delivery particles for transient in vitro and in vivo transgene expression, Human Gene Therapy Methods 27 (2016) 87–97.
[26] B. Su, A. Cengizeroglu, K. Farkasova, J.R. Viola, M. Anton, J.W. Ellwart, R. Haase, E. Wagner, M. Ogris, Systemic TNFalpha gene therapy synergizes with liposomal doxorubicine in the treatment of metastatic cancer, Mol. Ther. 21 (2013) 300–308.
[27] K. Müller, M. Ogris, H. Sami, Firefly Luciferase-Based Reporter Gene Assay for Investigating Nanoparticle-Mediated Nucleic Acid Delivery, Meth. ,Mol. Biol. (Clifton, N.J.) 1943 (2019) 227–239.
[28] N.D. Sonawane, F.C. Szoka Jr., A.S. Verkman, Chloride accumulation and swelling in endosomes enhances DNA transfer by polyamine-DNA polyplexes, J. Biol. Chem. 278 (2003) 44826–44831.
[29] N. Bäumer, J. Tiemann, A. Scheller, T. Meyer, L. Wittmann, M.E.G. Suburu, L. Greune, M. Peipp, N. Kellmann, A. Gumnior, C. Brand, W. Hartmann, C. Rossig, C. Müller-Tidow, D. Neri, C.A. Strassert, C. Rüter, P. Dersch, G. Lenz, H.P. Koeffler, W.E. Berdel, S. Bäumer, Targeted siRNA nanocarrier: a platform technology for cancer treatment, Oncogene 41 (2022) 2210–2224.
[30] T. Takahashi, K. Kono, T. Itoh, N. Emi, T. Takagishi, Synthesis of novel cationic lipids having Polyamidoamine Dendrons and their transfection activity, Bioconjug. Chem. 14 (2003) 764–773.
[31] T.L. Nascimento, H. Hillaireau, M. Noiray, C. Bourgaux, S. Arpicco, G. Pehau-Arnaudet, M. Taverna, D. Cosco, N. Tsapis, E. Fattal, Supramolecular organization and siRNA binding of hyaluronic acid-coated Lipoplexes for targeted delivery to the CD44 receptor, Langmuir 31 (2015) 11186–11194.
[32] B.A. Lobo, G.S. Koe, J.G. Koe, C.R. Middaugh, Thermodynamic analysis of binding and protonation in DOTAP/DOPE (1:1): DNA complexes using isothermal titration calorimetry, Biophys. Chem. 104 (2003) 67–78.
[33] T.L. Nascimento, H. Hillaireau, M. Noiray, C. Bourgaux, S. Arpicco, G. Pehau-Arnaudet, M. Taverna, D. Cosco, N. Tsapis, E. Fattal, Supramolecular organization and siRNA binding of hyaluronic acid-coated Lipoplexes for targeted delivery to the CD44 receptor, Langmuir 31 (2015) 11186–11194.
[34] E. Pozharski, R.C. MacDonald, Lipoplex thermodynamics: determination of DNA-cationic lipoid interaction energies, Biophys. J. 85 (2003) 3969–3978.
[35] H. Engelberg, Plasma heparin levels in normal man, Circulation 23 (1961) 578–581.
[36] J. Tang, R. Kuai, W. Yuan, L. Drake, J.J. Moon, A. Schwendeman, Effect of size and pegylation of liposomes and peptide-based synthetic lipoproteins on tumor targeting, Nanomedicine 13 (2017) 1869–1878.
[37] R.N. Majzoub, C.L. Chan, K.K. Ewert, B.F. Silva, K.S. Liang, E.L. Jacovetty, B. Carragher, C.S. Potter, C.R. Safinya, Uptake and transfection efficiency of PEGylated cationic liposome-DNA complexes with and without RGD-tagging, Biomaterials 35 (2014) 4996–5005.
[38] E.J. Sayers, S.E. Peel, A. Schantz, R.M. England, M. Beano, S.M. Bates, A.S. Desai, S. Puri, M.B. Ashford, A.T. Jones, Endocytic profiling of cancer cell models reveals critical factors influencing LNP-mediated mRNA delivery and protein expression, Mol. Ther. 27 (2019) 1950–1962.
[39] E. Figueroa, P. Bugga, V. Asthana, A.L. Chen, J. Stephen Yan, E.R. Evans, R. A. Drezek, A mechanistic investigation exploring the differential transfection efficiencies between the easy-to-transfect SK-BR3 and difficult-to-transfect CT26 cell lines, J. Nanobiotechnol. 15 (2017) 1–15.
[40] L. Ouyang, R. Shaik, R. Xu, G. Zhang, J. Zhe, Mapping surface charge distribution of single-cell via charged nanoparticle, Cells 10 (2021) 1519.
[41] F.D. Oliveira, M. Cavaco, T.N. Figueira, J. Valle, V. Neves, D. Andreu, D. Gaspar, M. A.R.B. Castanho, The antimetastatic breast cancer activity of the viral protein-derived peptide vCPP2319 as revealed by cellular biomechanics, FEBS J. 289 (2022) 1603–1624.
[42] S.G. Patel, E.J. Sayers, L. He, R. Narayan, T.L. Williams, E.M. Mills, R.K. Allemann, L.Y.P. Luk, A.T. Jones, Y.H. Tsai, Cell-penetrating peptide sequence and modification dependent uptake and subcellular distribution of green florescent protein in different cell lines, Sci. Rep. 9 (2019) 6298.
[43] M. Ogris, P. Steinlein, M. Kursa, K. Mechtler, R. Kircheis, E. Wagner, The size of DNA/transferrin-PEI complexes is an important factor for gene expression in cultured cells, Gene Ther. 5 (1998) 1425–1433.
[44] J. Wolfram, S. Nizzero, H. Liu, F. Li, G. Zhang, Z. Li, H. Shen, E. Blanco, M. Ferrari, A chloroquine-induced macrophage-preconditioning strategy for improved nanodelivery, Sci. Rep. 7 (2017) 13738.
[45] M. Sousa de Almeida, E. Susnik, B. Drasler, P. Taladriz-Blanco, A. Petri-Fink, B. Rothen-Rutishauser, Understanding nanoparticle endocytosis to improve targeting strategies in nanomedicine, Chem. Soc. Rev. 50 (2021) 5397–5434.
[46] K.G. de Bruin, C. Fella, M. Ogris, E. Wagner, N. Ruthardt, C. Brauchle, Dynamics of photoinduced endosomal release of polyplexes, J. Control. Release 130 (2008) 175–182.
[47] A. Taschauer, W. Polzer, S. Poschl, S. Metz, N. Tepe, S. Decker, N. Cyran, J. Scholda, J. Maier, H. Bloss, M. Anton, T. Hofmann, M. Ogris, H. Sami, Combined chemisorption and complexation generate siRNA Nanocarriers with biophysics optimized for efficient gene knockdown and air-blood barrier crossing, ACS Appl. Mater. Interfaces 12 (2020) 30095–30111.
[48] J.M. Harp, D.C. Guenther, A. Bisbe, L. Perkins, S. Matsuda, G.R. Bommineni, I. Zlatev, D.J. Foster, N. Taneja, K. Charisse, M.A. Maier, K.G. Rajeev, M. Manoharan, M. Egli, Structural basis for the synergy of 4′- and 2′-modifications on siRNA nuclease resistance, thermal stability and RNAi activity, Nucleic Acids Res. 46 (2018) 8090–8104.
[49] E.J. Sayers, S.E. Peel, A. Schantz, R.M. England, M. Beano, S.M. Bates, A.S. Desai, S. Puri, M.B. Ashford, A.T. Jones, Endocytic profiling of Cancer cell models reveals critical factors influencing LNP-mediated mRNA delivery and protein expression, Mol. Ther. 27 (2019) 1950–1962.
[50] Y. Guo, Q. Zhang, Q. Zhu, J. Gao, X. Zhu, H. Yu, Y. Li, C. Zhang, Copackaging photosensitizer and PD-L1 siRNA in a nucleic acid nanogel for synergistic cancer photoimmunotherapy, Sci. Adv. 8 (2022) eabn2941.
[53] F. Bellato, S. Feola, G. Dalla Verde, G. Bellio, M. Pirazzini, S. Salmaso, P. Caliceti, V. Cerullo, F. Mastrotto, Mannosylated polycations target CD206+- antigen presenting cells and mediate T-cell specific activation in cancer vaccination, Biomacromolecules 23 (2022) 5148–5163.